STUDY OF SOME THEORETICAL DESCRIPTIONS OF THE DEPENDENCE OF THE FRACTURE PARAMETERS ON THE SAMPLE SIZE★

DAN-ALEXANDRU IORDACHE*, VETURIA CHIROIU**, VIORICA IORDACHE*

* Physics Department, "Politehnica" University of Bucharest, Romania
** Institute for Solid Mechanics, Romanian Sciences Academy, Bucharest, Romania
* *E-mail:* daniordache2003@yahoo.com

Received December 21, 2004

The existing experimental data concerning the size effects on the fracture parameters [1] were analyzed, in order to check the validity of certain theoretical models. In this aim, the present work studied: a) the use of some statistical tests in order to point out and eliminate the "rough" errors, b) different theoretical models (*e.g.*, the Bazant's Size Effect Law [2], the Modified Size Effect Law [3], [4], and the Carpinteri's Multifractal Scaling Law (MFSL) [5]) of the fracture parameters of concrete specimen, c) the compatibility of the above studied theoretical models relative to the experimental data corresponding to some concrete or rock specimen, especially.

Key words: Size effects, fracture parameters, fractal dimension, multifractals, similitude.

1. INTRODUCTION

As it is well known, the mechanical response of a material to a state of stress is the result of many competing processes [as the dislocation generation and motion, grain-boundary sliding and migration, interplanar cleavage, segregation, self-diffusion, etc.] that originate at atomic scale, but have macroscopic consequences. That is why the description of such deformation and fracture phenomena require considerably more complex models than those existing in the continuum mechanics [particularly, the continuum mechanics models of the size effects, as the Bazant's one (SEL) [2] are able to describe accurately the size dependencies of the fracture parameters in narrow size regions (*e.g.* for $b_{max}/b_{min} \leq 4$), but they lead to predictions incompatible with the experimental results for wide size ranges (as $b_{max}/b_{min} \approx 30$ [28]).

On the other hand, these deformation and fracture phenomena are too complex to be approached usually by the present-day microscopic (atomistic

★ Paper presented at the 5th International Balkan Workshop on Applied Physics, 5–7 July 2004, Constanța, Romania.

Rom. Journ. Phys., Vol. 50, Nos. 7–8, P. 847–858, Bucharest, 2005

[29] or even large-scale molecular dynamics [30]) simulation techniques. That is why the descriptions of the fracture parameters by means of the similitude theory and/or of the fractal (self-similarity) theory present in following a high theoretical and technical interest.

Despite of the fact that it originates from Antiquity and the Medium Age (see *e.g.* the similitude criteria of Archimedes, Galileo Galilei, the first similitude theory theorem of Newton, etc), the modern theory of the physical similitude was elaborated mainly in the previous century.

As it concerns the main notion of the Fractals theory – that of *fractal dimension*, some elements in this direction appeared by means of the works of Bouligand, Richardson, and Rogers. Short time after his well-known editions concerning the Fractals theory [6], Mandelbrot *et al.* [11] studied the use of some effective fractal dimensions (the "slit island" method, the spectral method and the "impact energy" fractal dimension) in order to describe the fracture surface and parameters of some metals and alloys. The work [11] illustrated the possibilities to use the Fractals theory in order to study the fracture phenomena in different materials, but this work was widely criticized for different reasons.

A considerably improved fractal approach of the fracture phenomena was accomplished by means of the Carpinteri's models [8, 9], which – using also multifractal and similitude descriptions – succeeded to describe accurately even the size dependence of the fracture parameters in wide size ranges ($b_{max}/b_{min} \approx$ ≈ 30 [28]).

The applications in Physics of the mathematical theory of the *ideal* fractals [6] need a good understanding of this concept, from the physical point of view. A first attempt in this direction was done recently by M. Rybaczuk and W. Zielinski [7]. Unfortunately, the works [7] do not refer also to the presence of the measurement errors, which are specific to the real Physics studies. Or, these errors are present and even they are relatively large [1].

In frame of their well-known paper [11], B. B. Mandelbrot and his collaborators claimed that "the value of (the fractal dimension) D decreases smoothly with an increase of the impact energy" and "D is shown to be a measure of toughness in metals". Unfortunately, B.B. Mandelbrot *et al.* did not mention the accuracy of their experimental data and they did not tried to accomplish a study of the compatibility of their hypothesis (concerning the linear relationships between the fracture parameters and the fractal dimension) relative to the existing experimental data (moreover, Mandelbrot stated [12] that the frequent use of numbers by physicists is a mistake and it would be better if they could focus mainly on the study of plots).

Taking into account that: a) the correlation coefficients indicate only the degree of proximity of the confidence domains centers relative to the studied regression curve, b) for high accuracy of the experimental data, the theoretical

relations are not more compatible with these experimental data, even for high values of the correlation coefficient (see Table 2), c) the existence for concrete of several experimental data [1, 14] referring to the size dependence of the fracture parameters, as well as of some (multi)fractal descriptions of these effects [8, 9], *this work will accomplish a numerical analysis of these existing experimental data, as well as of the compatibility of the multifractal and similitude expressions of the fracture parameters relative to the analyzed experimental results.*

2. NUMERICAL ANALYSIS OF SOME EXPERIMENTAL DATA REFERRING TO THE SIZE DEPENDENCE OF FRACTURE PARAMETERS OF SOME CONCRETE AND ROCK SPECIMEN

The study of the compatibility of some theoretical relations relative to the analyzed experimental data needs the previous elimination of the rough errors, as well as the evaluation of the square mean errors affecting the studied experimental results. In this aim, starting from the zero-order evaluation of the square mean error: $s(x)=\sqrt{\frac{1}{N-1}\sum_{i=1}^{N}\left(x_i-\tilde{x}_N\right)^2}$, we evaluated the reduced errors $z_i=\frac{x_i-\tilde{x}_N}{s\left(x_i\right)}$ and we used the Chouvenet's criterion [15], eliminating the individual values x_i whose absolute values of the reduced errors were larger than the Chouvenet's threshold:

$$z_{thr.}=\arg\varphi\left(\frac{2N-1}{4N}\right), \tag{1}$$

where argφ is the inverse function (argument) of the integral of errors:

$$\varphi(z)=\frac{1}{\sqrt{2\pi}}\int_0^z \exp\left(-\frac{z^2}{\mathrm{d}z}\right)\mathrm{d}z. \tag{2}$$

The use of this procedure to the study of the numerical values of some fracture parameters [1, 14], pointed out that the individual values δ_u= 7.7 μm and δ_u = 9.7 μm, respectively, of the critical strain corresponding to some specimens of size b = 20 cm of dry and wet concrete [1], respectively are roughly erroneous. After the elimination of these individual values, the mean values $\tilde{x}_{Nc}$ and the square mean errors $s_c(x)$ were recalculated for the compatible individual values.

The obtained results corresponding to the tensile strength σ_N (MPa), critical strain (deformation) w_u (μm) and to the fracture energy G_F (N/m) for specimens of different natures (materials) and sizes were synthesized in Table 1.

Table 1

Average values and standard errors corresponding to some existing experimental data concerning the main fracture parameters of some concrete and rock specimens, respectively

Reference	Material	Specimen size, cm (samples number)	σ_N [MPa]		w_u [μm]		G_F [*N/m*]	
			Average value $\tilde{\sigma}_N$	Relative Standard Error, %	Average value $\tilde{w}_u$	Relative Standard Error, %	Average value	Relative Standard Error, %
Carpinteri [14]	Concrete	2.5 (4)	4.7925	4.679	–	–	146.25	15.58
		5.0 (7)	4.56	5.315	–	–	257.57	22.002
		10.0 (7)	4.3543	3.926	–	–	236.25	10.964
		20.0 (4)	3.80	9.755	–	–	158.0	Insuffi–cient Data
		40.0 (4)	3.7225	6.636	–	–	214.0	47.581
M.R.A. van Vliet [1]	DRY Concrete	5.0 (10)	2.536	16.217	1.64	42.167	97.045	12.185
		10.0 (4)	2.9725	6.278	5.20	11.103	125.70	14.299
		20.0 (7)	2.750	7.674	9.833*	6.674*	124.243	10.918
		40.0 (5)	2.298	4.028	14.78	10.051	125.22	10.937
		80.0 (4)	2.0725	5.914	22.025	9.584	142.30	7.243
		160.0 (4)	1.8575	8.674	44.40	14.038	141.10	7.212
M.R.A. van Vliet [1]	WET Concrete	5.0 (5)	2.174	11.585	2.180	24.999	91.48	20.914
		10.0 (5)	2.230	5.663	4.10	5.064	99.66	10.196
		20.0 (5)	2.476	6.142	8.025*	3.721*	88.92	13.542
		40.0 (4)	2.365	2.502	15.725	4.798	100.367	9.825
M.R.A. van Vliet [1]	RED FELSER SAND–STONE	5.0 (2)	2.450	Insuffi–cient Data	28.45	18.641	76.75	6.910
		10.0 (3)	1.2167	4.527	44.167	3.074	111.333	3.281
		20.0 (3)	1.010	3.430	69.20	13.577	93.80	4.687
		40.0 (3)	0.960	3.125	156.80	5.644	135.067	9.640
		80.0 (3)	1.300	34.675	263.70	2.842	143.350	11.592
		160.0 (3)	1.200	35.424	434.70	16.303	81.80	25.533

* These values were obtained after the elimination of rough errors.

3. EXISTING AND NEWLY DERIVED THEORETICAL AND SEMIEMPIRICAL RELATIONS INVOLVING FRACTURE PARAMETERS AND (EXPLICITLY OR IMPLICITLY) THE FRACTAL DIMENSIONS

Taking into account that: a) during the fracture processes, there appear – in the fracture region – some voids, cracks, etc, the physical dimension of the effective (normalized) fractal cross-section area A_σ^* corresponding to the tensile

strength is somewhat less than 2: $D_\sigma = 2 - d_\sigma$, where d_σ is the corresponding decrement, b) the energy necessary to produce the fracture is dissipated in a 3D-region around the fracture cross-section, the effective (normalized) cross-section area A_G^* corresponding to the fracture energy G_F is somewhat larger than 2: $D_G = 2 + d_G$, where d_G is the corresponding fractal increment. It results that the physical dimensions of the tensile strength σ_u $\left(= \frac{F}{A} = \sigma_u^* \frac{A_\sigma^*}{A}\right)$ and of the fracture energy G_F $\left(= \frac{W}{A} = G_F^* \frac{A_G^*}{A}\right)$ can be expressed as:

$$\left[\sigma_u\right] = \left[\sigma_u^*\right] \cdot \left[\frac{A_\sigma^*}{A}\right] = \left[\sigma_u^*\right] \cdot L^{-d_\sigma}, \quad \left[G_F\right] = \left[G_F^*\right] \cdot \left[\frac{A_G^*}{A}\right] = \left[G_F^*\right] \cdot L^{d_G}, \tag{3}$$

where σ_u^* and G_F^* are the normalized (size independent) tensile strength and fracture energy, respectively. According to the definition of the similar states Σ, Σ′, by means of the values of their uniqueness parameters U_i and of the other state parameters P [16]: $\frac{P}{P'} = \prod_{i=1}^{n_U} \left(\frac{U_i}{U_i'}\right)^{\alpha_i}$, if: $[P] = \prod_{i=1}^{n_U} [U_i]^{\alpha_i}$, it results that: $\frac{\sigma_u}{\sigma_u'} = \left(\frac{b}{b'}\right)^{-d_\sigma}$ and: $\frac{G_F}{G_F'} = \left(\frac{b}{b'}\right)^{d_G}$, therefore:

$$\ln \sigma_u = \ln \sigma_u^* - d_\sigma \ln b, \quad \text{and:} \quad \ln G_F = \ln G_F^* + d_G \ln b. \tag{4}$$

Because the studies [8, 9], [13, 14] point out a considerable curvature of the plots $\ln \sigma_u$, $\ln G_F = f(\ln b)$ (Table 2 indicates also considerably different values of the effective fractal dimensions for specimens of different sizes), there were derived some theoretical and semiempirical expressions of the tensile strength σ_u and of the fracture energy G_F as that of Bazant [2–4]:

$$\sigma_u = \frac{\sigma_{u0}}{\sqrt{1 + \frac{b}{l_{\sigma B}}}}, \tag{5}$$

and those of Carpinteri [8, 9]:

$$\sigma_u = \sigma_{u\infty} \sqrt{1 + \frac{l_{\sigma C}}{b}} \quad \text{and:} \quad G_F = \frac{G_{F\infty}}{\sqrt{1 + \frac{l_{GC}}{b}}}, \tag{6}$$

where $l_{\sigma B}$, $l_{\sigma C}$ and l_{GC} are some different (specific) characteristic lengths. One

Table 2

Definitions of the main effective mechanical fractal dimensions

Index	Name of the fractal dimension	DEFINITION	Reference(s)
1	Impact energy	$E_i = E_{i0} - (D_e - 2)E_{if}$, where E_{i0}, E_{if} are parameters specific to the fracture surfaces of each metal (alloy)	[11]
2	Fatigue Parameters	$D_f = \frac{b+2}{b+1}$, where: $b = \frac{\log(\varepsilon_t / 2)}{\log N_f}$, while $\varepsilon_t = \varepsilon_e + \varepsilon_p$ is the total strain when the plastic strain ε_p is equal to the elastic one (ε_e) and N_f = number of fatigue cycles at failure	[23]
3	Crack Cavity Propagation	$D_c = 1 + \frac{\log(W_0 / W)}{\log(W_0 / d)}$, where W is the length of a characteristic element of the fractal associated to the irregular path of crack cavity propagation, W_0 is the distance between the ends of this element and d is the distance between the opposite faces of the grain	[24]
4	Cut-off method	Spectral (frequency) analysis after the elimination of the long wavelength components, for *2D* roughened surfaces	[25]
5	Distribution method	$\log N = \log N_1 - \frac{D}{D_i}\log p$, where N is the number of particles of size p and D_i is the dimension of the ideal geometrical element (1 for curves, 2 for surfaces, etc)	[26, 27]
6	Tensile strength	$\log \sigma_u = \log \sigma_{u0} + (D_\sigma - 2)\log b$, where σ_u is the tensile strength and b is the specimen size	[5]
7	Fracture energy	$\log G_F = \log G_{F0} + (D_G - 2)\log b$, where G_F is the fracture energy corresponding to a specimen of size b	[5]
8	Critical strain	$\log w_c = \log \varepsilon_c + D_w \log b$, where w_C is the crack opening displacement at the critical stress, for a specimen of size b	[28]

finds that if $l_{\sigma B} << b << l_{\sigma C}$, both theoretical expressions of Bazant (5) and Carpinteri (6) of the tensile strength converge towards the proportionality: $\sigma_u \propto b^{-1/2}$. Using: a) the similitude criteria $1 + \frac{b}{l_{chB}}$ and $1 + \frac{l_{chC}}{b}$, specific to the theoretical models of Bazant [2–4] and Carpinteri [8, 9], respectively, b) the condition of homogeneity of these similitude criteria in frame of the relationships as:

$$G_F^* b^{d_G} = G_F = \int_0^{w_c} \sigma \cdot \mathrm{d}w = b^{1-d_w-d_\sigma}, \tag{7}$$

where d_w is the strain fractal decrement, c) the characteristic convergence

towards proportionality with $b^{\pm 1/2}$ of the Bazant's and Carpinteri's models for $l_{\sigma B} << b << l_{\sigma C}$, we obtained *3 new semiempirical relations of the size-effects on fracture parameters*: 2 of the Bazant's type and one of the Carpinteri's type:

$$G_F = G_{F0}\sqrt{1+\frac{b}{l_{GB}}}, \quad w_f = w_{f0}\left(1+\frac{b}{l_{wB}}\right), \quad w_f = \frac{w_{f\infty}}{1+\frac{l_{wC}}{b}}, \tag{8}$$

where $w_{f\infty}$ is the upper threshold of the critical fracture strain. From relation (7), it results that the fractal increment d_G is related to the fractal decrements d_σ and d_w by means of the expression:

$$d_G = 1 - d_\sigma - d_w. \tag{9}$$

4. PROCEDURE TO STUDY THE COMPATIBILITY OF THEORETICAL RELATIONS RELATIVE TO THE EXISTING EXPERIMENTAL DATA

Starting from the obtained experimental results referring to the fracture parameters (Y) and to the specimen sizes (X), the confidence ellipses associated to the most probable individual values corresponding to the studied state i (x_{imp}, y_{imp}, $i = 1, n$) for some chosen confidence levels L are obtained [17–19]:

$$\left(\frac{x-x_{imp}}{s(x_i)}\right)^2 + \left(\frac{y-y_{imp}}{s(y_i)}\right)^2 - 2r_i\left(\frac{x-x_{imp}}{s(x_i)}\right)\left(\frac{y-y_{imp}}{s(y_i)}\right) = f_2(L) = \\ = 2\left(1-r_i^2\right)\ln L, \tag{10}$$

where: $r_i = \dfrac{Cov_i(x,y)}{s(x_i)s(y_i)}$ is the correlation coefficient of the pairs of individual values (belonging to the state i) of parameters X, Y, and $Cov_i(x,y) = \left\langle (x-x_{imp})(y-y_{imp}) \right\rangle$ is the covariance of these parameters for the state i.

Let $Y = f(X)$ be the studied theoretical (or semiempirical) relation. In order to evaluate the material parameters (*e.g.* the characteristic lengths l_{ch} and the asymptotic parameters p_0 of Bazant [2–4] or p_∞ of Carpinteri [8, 9]) involved by the theoretical relation $y = f(x)$, avoiding the unpleasant numerical phenomena of oscillations or divergence, we started from the classical algorithms [20, 21] of the gradient method, and we used a new (improved) version of the damping procedure of Mei and Morris [22]. In this aim, we generalized the damping factor λ [22] as a diagonal matrix $\overline{\overline{\Lambda}}$ and we used for

the correction vector $\bar{C}^{(I)}$ of the material parameters in frame of the *I*-th successive iteration the expression:

$$\bar{C}^{(I)} = -\bar{\bar{\Lambda}}\left(\bar{\bar{J}}^{(I)^T} \cdot \bar{\bar{W}} \cdot \bar{\bar{J}}^{(I)}\right)^{-1} \cdot \bar{\bar{J}}^{(I)} \cdot \bar{\bar{W}} \cdot \bar{D}^{(I)}, \tag{11}$$

where: $J_{ij}^{(I)} = \dfrac{\partial t_{calc}^{(I)}}{\partial p_j}$ are the elements of the jacobian $\bar{\bar{J}}^{(I)}$ (in iteration *I*), $W_{ij} = \dfrac{1}{t_{\exp.j}^2}\delta_{ij}$ are the elements of the (diagonal) matrix $\bar{\bar{W}}$ of weights, $\bar{D}^{(I)} = \bar{t}_{calc.}^{(I)} - \bar{t}_{\exp}$ is the vector of the deviations of the calculated (in iteration *I*) values of the test parameters (*e.g.* the fracture ones) relative to the experimental values, while: $\bar{\bar{\Lambda}} = \lambda_i \delta_{ij}$, the damping factors (< 1) being chosen in order to ensure a monotonic convergence of the iterative (for successive approximations) procedure of the gradient method. An algorithm intended to the evaluation of the coordinates x_{ti}, y_{ti} of the tangency point of a confidence ellipse belonging to the family (1), to the theoretical relation plot $Y = f(X)$ (see Fig. 1), was also elaborated by us in frame of the work [10]. Starting from the coordinates x_{ti}, y_{ti}, the error risk q_i at the rejection of the compatibility of the studied theoretical relation $Y = f(X)$ relative to the "local" experimental data referring to the "state" *i* was estimated as:

$$q_i = 1 - \exp\left\{-\frac{1}{2\left(1-r_i^2\right)}\left[\left(\frac{x_{ti}-x_{imp}}{s\left(x_i\right)}\right)^2 + \left(\frac{y_{ti}-y_{imp}}{s\left(y_i\right)}\right)^2 - 2r_i\left(\frac{x_{ti}-x_{imp}}{s\left(x_i\right)}\right)\left(\frac{y_{ti}-y_{imp}}{s\left(y_i\right)}\right)\right]\right\}. \tag{12}$$

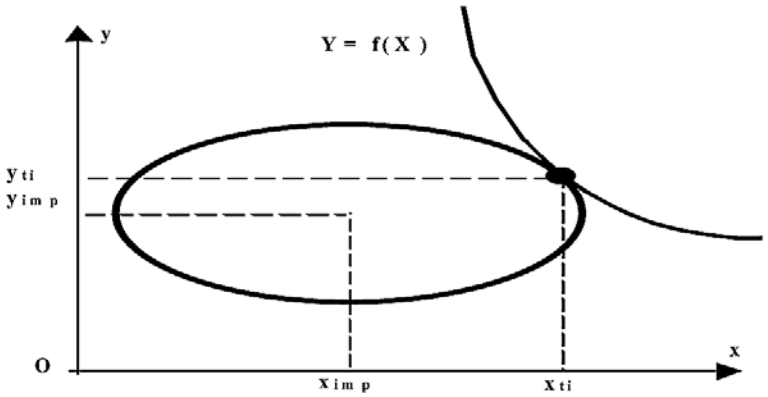

Fig. 1

As the error risk q_i is larger than 2%, or it is less than 0.1%, the compatibility of the studied theoretical relation $Y = f(X)$ relative to the local experimental data referring to the "state" i has to be accepted, or it has to be rejected.

5. OBTAINED RESULTS AND CONCLUSIONS

Taking into account that there are different effective mechanical fractal dimensions which are used to study the mechanical processes (and the fracture ones, frequently), we synthesized also – in Table 2 – the definitions and main features of the main such parameters.

The obtained results concerning the compatibility of the (multi)fractal (Carpinteri's) expressions and of the classical elasticity theory (Bazant's) expressions of the size-effects presented by the tensile strength σ_N, the fracture energy G_F and by the critical strain w_u relative to the existing experimental data are synthesized in frame of Table 3. The analysis of the results from Table 3 points out: a) the "local" incompatibility of the studied theoretical models with the experimental data (TM/ED) corresponding to the tensile strength of the Red Felser Sandstone for 3 or 4 sizes (from the 6 studied ones) of the studied specimens, the Carpinteri's expression being though somewhat more accurate, b) the compatibility TM/ED for Dry Concrete specimens, the Bazant's description being somewhat more accurate, c) the compatibility TM/ED for Wet Concrete, but with strange (negative) values of the characteristic lengths, d) the compatibility TM/ED for G_F, with somewhat better accuracy and physical meaning of the values of the characteristic lengths obtained by means of Carpinteri's model for the Red Felser Sandstone and Dry Concrete specimens, e) the compatibility TM/ED for G_F, with somewhat equal accuracy of both studied models for the Wet Concrete, f) the compatibility TM/ED with somewhat better accuracy (excepting the van Vliet's results for Dry Concrete) of Bazant's type description of $w_u(b)$, g) unlike the characteristic lengths corresponding to the σ_N and G_F descriptions, when: $b \sim l_{chCarpinteri} << l_{chBazant}$, for the critical strain: $b \sim l_{chBazant} << l_{chCarpinteri}$, h) the rather broad ranges of fractal dimension values corresponding to the studied fracture surfaces [ratios of the extreme values corresponding to the fractal increment (or decrement, respectively) between 7.13 and 31.94 (see Table 3)].

The accomplished study allows the obtainment of the following conclusions: a) despite of its fruitful qualitative contribution (which allowed the derivation of Carpinteri's relations) of the Fractal Theory to the description of the size effects on fracture parameters, itself this theory cannot ensure always accurate results

Table 3

Study of the compatibility with experimental results of the main theoretical models of the size-effects on fracture parameters

Specimen (Ref.)	Range of sizes, dm Theoret. model	Range of fractal dimensions	Ratio of extreme values of Increment	σ_{ch} [MPa]	l_{ch} [dm]	Average Standard Error (%)	Correlation coefficient, r	Minimal Rejection Risks, % (for Size)
Red Felser Sandstone (RFS) [1]	0.5...16 [7–9]	1.6747... 1.9725	11.831	1.02726	9.31076	20.152	0.8262	10^{-10}; 0.01% for b = = 0.5...4 dm
RFS [1]	0.5...16 [4–6]	1.99896.. 1.99997	31.941	1.15839	77082.17	24.4132	0.4966	10^{-36}; 0.01% 0.5, 2&4 dm
Dry Concrete (DryC) [1]	0.5...16 [7–9]	1.76495.. 1.98651	17.427	2.0753	4.43573	12.2226	0.5881	3.71%;1 dm 9.68%;2 dm
Dry C. [1]	0.5...16 [4–6]	1.71015.. 1.97934	14.0293	2.7873	116.005	6.3232	0.9094	27.92% for b = 2 dm
Wet Concrete (WetC) [1]	0.5...4 [7–9]	2.01381.. 2.13695	9.9172	2.43535	–1.075	2.8195	0.8216	78.07% for b = 2 dm
Wet C. [1]	0.5...4 [4–6]	2.01054 ...2.0989	9.3845	2.21002	–242.225	3.8878	0.6020	54.06% for b = 2 dm
Concrete [14]	0.25...4 [7–9]	1.78465.. 1.97743	9.5395	3.74006	1.8913	4.0605	0.9104	27.20% for b = 1 dm
Concrete [14]	0.25...4 [4–6]	1.77875 ...1.9764	9.3627	4.77456	50.3977	3.6157	0.9420	81.12% for b = 2 dm
Fractal model: $G_F = G_{F\infty}/\sqrt{1+l_{ch}/b}$ [8, 9]				G_F, N/mm	Bazant's model: $G_F = G_{F0}\sqrt{1+b/l_{ch}}$ [2–4]			
RFS [1]	0.5...16 [7–9]	2.00918 ...2.1872	20.39	105.967	2.9927	20.548	0.4948	3.2×10^{-4} % for b = 1 dm
RFS [1]	0.5...16 [4–6]	2.00024 ...2.0076	31.5445	97.9466	10371.88	22.560	–0.0449	3.33×10^{-2} % for b = .5 dm
Dry C. [1]	0.5...16 [7–9]	2.01522 ...2.2506	16.464	141.569	5.02335	4.748	0.9175	83.5% for b = 4 dm
Dry C. [1]	0.5...16 [4–6]	2.01282 ...2.2285	17.8305	110.545	190.047	8.9202	0.7447	45.0%, for b = 0.5 dm
Wet C. [1]	0.5...4 [7–9]	2.00589 ...2.0435	7.3903	96.684	0.47694	5.045	0.3325	85.93% for b = 2 dm
Wet C. [1]	0.5...4 [4–6]	2.00868 ...2.0619	7.1330	91.7035	282.993	4.812	0.4470	82.26% for b = 1 dm
Concrete [14]	0.25...4 [7–9]	2.01612 ...2.1738	10.7854	202.5156	1.33225	20.28	0.2760	20.65% for b = 1 dm
Concrete [14]	0.25...4 [4–6]	1.99695 ...1.9998	16.094	172.785	–6592.37	22.451	–0.0164	4.91% for b = 1 dm

(continues)

Table 3 (continued)

Specimen (Ref.)	Range of sizes, dm Theoret. model	Range of fractal dimensions	Ratio of extreme values of Increment	σ_{ch} [MPa]	l_{ch} [dm]	Average Standard Error (%)	Correlation coefficient, r	Minimal Rejection Risks, % (for Size)
Fractal model: $w_u = w_{u\infty}/(1+l_{ch}/b)$ [8, 9]				w_u [μm]	Bazant's type: $w_u = w_{u0}(1+b/l_{ch})$ [2–4]			
RFS [1]	0.5...16 [7–9]	1.60928 ...1.9804	19.8877	1096.419	249.504	12.468	0.9990	36.94% for b = 1 dm
RFS [1]	0.5...16 [4–6]	1.5096 ...1.9708	16.7976	14.1474	4.81156	8.6568	0.9228	1.826% for b = 4 dm
Dry C. [1]	0.5...16 [7–9]	1.46592 ...1.9654	15.4439	73.8192	139.58	24.8294	0.9802	6.987% for b = 8 dm
Dry C. [1]	0.5...16 [4–6]	1.53402 ...1.9735	17.5546	1.40981	4.3630	37.8788	0.9940	1.1532% for b = 2 dm
Wet C. [1]	0.5...4 [7–9]	1.9747... 1.99677	7.82281	633.38	1541.08	3.22085	0.9999	92.44% for b = 4 dm
Wet C. [1]	0.5...4 [4–6]	1.89012 ...1.9848	7.23083	0.23927	0.61722	0.2932	0.9999	99.405% for b = 2 dm

concerning the fracture parameters corresponding to specimens of different dimensions, b) it seems that the fractal character of fracture surfaces and the (classical) elasticity theory implications on the size-effects of fracture parameters represent cooperative processes, the most accurate descriptions implying (generally) contributions of both these factors, *e.g.*:

$$\sigma_N(b) = \frac{\sigma_{0B}}{\sqrt{1+b/l_{\sigma B}}} + \sigma_{\infty C}\sqrt{1+\frac{l_{\sigma C}}{b}}. \tag{13}$$

REFERENCES

1. M. R. A. van Vliet, Ph. D. Dissertation, Tehnical University of Delft, January 31, 2000.
2. Z. P. Bazant, Journal of Engineering Mechanics, ASCE, 110, 1984, p. 518.
3. J. K. Kim, S. H. Eo, Magazine of Concrete Research, 42, 1990, p. 233.
4. Z. P. Bazant, M. T. Kazemi, T. Hasegawa, J. Mazers, ACI Materials Journal, 88, 1991, p. 325.
5. A. Carpinteri, Mechanics of Materials, 18, 1994, p. 89.
6. B. B. Mandelbrot, The Fractal Geometry of Nature, W. H. Freeman, San Francisco, 1982.
7. a) M. Rybaczuk, W. Zielinski, Chaos, Solitons and Fractals, 12, 2001, p. 2517; b) ibid., Chaos, Solitons and Fractals, 12, 2001, p. 2536.
8. A. Carpinteri, F. Ferro, Materials and Structures, 31, 1998, p. 303.
9. A. Carpinteri, B. Chiaia, Materials and Structures, 29, 1996, p. 259.
10. D. Iordache, On the Compatibility of some Theoretical Models relative to the Experimental Data, *Proceedings of the 2nd Colloquium Mathematics in Engineering and Numerical Physics*, Bucharest, April 2002, part 2, 169–176.
11. B. B. Mandelbrot, D. E. Passoja, A. J. Paullay, Fractal character of fracture surfaces of metals, *Nature*, 6 (April 19) 1984, 721–722.

12. B. B. Mandelbrot, Opinions, *Fractals*, 1(1), 1993, 117–123.
13. P. P. Delsanto, D. Iordache, Șt. Pușcă, Study of the Correlations between different effective fractal dimensions used for fracture parameters descriptions, *First South-East European Symposium on Interdisciplinary approaches in fractal analysis*, Bucharest, May 7–10, 2003
14. A. Carpinteri, F. Ferro, Scaling behaviour and dual renormalization of experimental tensile softening responses, *Materials and Structures*, 31, 1998, 303–309.
15. L. Jánossy, Theory and Practice of the Evaluation of Measurements, Oxford University Press,1965.
16. A. A. Gukhman, Introduction to the Theory of Similarity, Academic Press, New York , 1965.
17. W. T. Eadie, D. Drijard, F. E. James, M. Roos, B. Sadoulet, Statistical Methods in Experimental Physics, North-Holland Publ. Company, Amsterdam-New York-Oxford, 1982.
18. *** Handbook of Applicable Mathematics, chief editor Walter Ledermann, volume VI: Statistics, John Wiley & Sons, New York, 1984.
19. P. W. M. John, Statistical Methods in Engineering and Quality Assurance, John Wiley & Sons, New York, 1990.
20. K. Levenberg, Quart. Appl. Math., 2, 1944, p. 164.
21. D. W. Marquardt, J. of Soc. Industr. Appl. Math., 11, 1963, p. 431.
22. Z. Mei, J. W. Morris jr., J. Nucl. Instrum. Methods in Phys. Res., 6, 1990, p. 371.
23. R. E. Williford, Fractal Fatigue, *Scripta Metallurgica et Materialia,* 25, 1991, 455–460.
24. X. Jiang, J. Cui, L. Ma, *Acta Metallurgica et Materialia,* 40, 1992, 1267.
25. I. Shimizu, T. Abbe, Surface Roughening and Fractal Dimension during Plastic Deformation of Polycrystalline Iron, *JSME International Journal,* series A, 37(4) 1994, 403–411.
26. D. L. Turcotte, Fractals and Chaos in Geology and Geophysics, Cambridge Univ. Press, 1992.
27. A. Carpinteri, B. Chiaia, P. Cornetti, A scale-invariant cohesive crack model for quasi-brittle materials, *Engineering Fracture Mechanics,* 69, 2002, 207–217.
28. A. Carpinteri, B. Chiaia, Multifractal Scaling Laws in the Breaking Behaviour of Disordered Materials, *Chaos, Solitons & Fractals,* 8(2) 1997, 135–150.
29. F. Cleri, S. R. Phillpot, D. Wolf, S. Yip, Atomistic Simulations of Materials Fracture and the Link between Atomistic and Continuum Length Scales, *J. Am. Ceram. Soc.,* 81(3) 1998, 501–516.
30. S. R. Phillpot, P. Keblinski, D. Wolf, Synthesis and Characterization of a Polycrystalline Ionic Thin Film by Large-Scale Molecular-Dynamics Simulation, *Interface Science*, 7, 1999, 15–31.